

Scientific paper

Conjugate imaging riometer observations at polar cusp/cap stations: A daytime absorption event for a specific change of solar wind conditions

Masanori Nishino¹, Hisao Yamagishi², Natsuo Sato², Yozo Murata³,
Ruiyuan Liu⁴, Peter Stauning⁵ and Jan A. Holtet⁶

¹*Solar-Terrestrial Environment Laboratory, Nagoya University, Honohara, Toyokawa 442-8507*

²*National Institute of Polar Research, Kaga 1-chome, Itabashi-ku, Tokyo 173-8515*

³*Department of Polar Science, the Graduate University for Advanced Studies,
Kaga 1-chome, Itabashi-ku, Tokyo 173-8515*

⁴*Polar Research Institute of China, 451 Shang Chuan Road, Shanghai, 200129, China*

⁵*Danish Meteorological Institute, Lyngbyvej 100, Copenhagen, Denmark*

⁶*Department of Physics, University of Oslo, Oslo, Norway*

Abstract: Using the imaging riometers at Ny-Ålesund and Danmarkshavn in the Arctic region, and Zhongshan in Antarctica, a daytime absorption spike event was observed at both hemispheric stations in the post-noon (13–15 h MLT) on August 3, 1997. The conjugate absorption spikes with a quasi-periodic feature were associated with the sequence of solar wind dynamic pressure pulses during northward interplanetary magnetic field (IMF). In particular, the absorption spike associated with the steep pressure increase and the synchronous short-period southward IMF change exhibited a time difference (~ 1 min) between the occurrences in the two hemispheres. From comparison between the absorption images and simultaneous aurora all-sky images at Zhongshan, it is recognized that the absorption spike shows a feature of small-scale enhancement with fast eastward motion in the large-scale absorption extending by about 1000 km in longitude and about 50 km in latitude. Ground geomagnetic variations at the high-latitude stations in the both hemispheres showed good response to the solar wind pressure pulse sequence. These observational results indicate that magnetic compressional waves driven by the solar wind pressure pulses could stimulate energetic electrons populating in the outer magnetosphere and thus the electrons could precipitate into the polar cleft ionosphere in both hemispheres due to intensification of upward region-I field aligned currents near the duskside magnetopause.

1. Introduction

The solar wind flow around the Earth's magnetosphere is by no means in a steady state but is characterized by major changes of the interplanetary magnetic field (IMF) and its plasma velocity as well as its plasma density. The response of the dayside magnetosphere to sudden changes of solar wind conditions is a major dynamic feature of the solar wind interaction with the Earth's magnetosphere.

Glassmeier and Heppner (1992) illustrated schematically magnetopause current layer

perturbations associated with solar wind pressure pulses and magnetic merging (reconnection). Pressure enhancement and magnetic merging events result in localized increases of the local magnetopause current density. From current continuity at the boundary, field-aligned currents (FACs) flow out of the auroral ionosphere, carrying magnetospheric electrons into the dayside ionosphere. Therefore, ground-based auroral observation in the polar cusp/cleft region is a significant remote sensing technique for studying transfer of momentum and energy from the solar wind to the magnetosphere and the polar ionosphere.

Sandholt *et al.* (1994) revealed that strong, isolated enhancements in solar wind dynamic pressure gave rise to equatorward shifts of the cusp/cleft aurora at Ny-Ålesund (geomag. lat., 76°) during southward ($B_z < 0$) and westward ($B_y < 0$) IMF. Farrugia *et al.* (1995) demonstrated a series of transient auroral emissions in the 1300–1600 MLT sector using the daytime auroral observations at Ny-Ålesund. The IMF showed a strong westward ($B_z \ll 0$) and a small northward or zero B_y . They interpreted the emissions in terms of modulations in the reconnection rate at the dayside magnetopause, stimulated by the arrival at Earth of upstream dynamic pressure pulses of the solar wind. Sandholt *et al.* (1996) demonstrated impulsive auroral emissions associated with the arrival of the interplanetary shock and with an IMF directional discontinuity during northward B_z . The transient form with strong green-line emissions at the equatorward boundary of the preexisting aurora showed an equatorward shift of about 100 km south of the zenith over Ny-Ålesund. Thus, as a next step of the dayside aurora studies, the topology of the magnetosphere when the reconnection region maps to the ionospheric projection of the boundary between open and close magnetic field-lines is required. This suggests a necessity of conjugate observations between high-latitude stations in the northern and southern hemispheres.

However, optical observations of auroral particle precipitation have limitations due to climate and sunlit conditions, in particular, simultaneous optical observations between high-latitude stations in the both hemispheres are nearly impossible. By contrast, measurement of ionospheric absorption of cosmic radio signals using a riometer (Relative Ionospheric Opacity meter) is always useful for detecting auroral particle precipitation without these limitations.

An imaging riometer for ionospheric study (IRIS) which is capable of measuring the spatial scale, shape and movement of absorption events, was initially deployed at South Pole station, Antarctica (invariant latitude -74°) in January 1988 (Detrick and Rosenberg, 1990), and since then multiple IRIS instruments have been installed in the Arctic region (*e.g.*, Stauning *et al.*, 1992; Nishino *et al.*, 1993) and in Antarctica (*e.g.*, Nishino *et al.*, 1998). Using the IRISs at Ny-Ålesund/Longyearbyen in Svalbard and Zhongshan station in Antarctica, a conjugate relationship of nighttime absorption events has been discussed in terms of the east-west component (B_y) of the IMF (Nishino *et al.*, 1998).

This paper presents in turn a daytime absorption event observed by the IRISs at the hemispheric high-latitude stations. The IRIS data used are from Ny-Ålesund in Svalbard, Danmarkshavn in Greenland and at Zhongshan station in Antarctica. A characteristic feature of the event is an association with a specific change of solar wind dynamic pressure and IMF. Solar wind parameters from the WIND satellite, aurora all-sky camera data at Zhongshan and ground geomagnetic data at high-latitude stations are used for examination of the conjugate relationship and for discussion of aurora particle precipitations, as a case study.

Table 1. Geographical coordinates of Danmarkshavn (DMH), Ny-Ålesund (NYA) and Zhongshan (ZHS) and their corrected geomagnetic latitudes, approximate magnetic-noon and total magnetic field according to the IGRF model.

Stations	Geographical coordinates	Corrected geomag. latitude	Eccentric dipole magnetic noon	Total magnetic field
Danmarkshavn(DMH)	76.77N, 18.66W	77.26	1036 UT	53660 nT
Ny-Ålesund (NYA)	78.92N, 11.92E	76.05	0847 UT	53959 nT
Zhongshan (ZHS)	69.37S, 76.38E	-74.52	1015 UT	53733 nT

Table 1 gives the geographical coordinates of Danmarkshavn (DMH), Ny-Ålesund (NYA) and Zhongshan (ZHS) and their corrected geomagnetic latitudes, approximate magnetic noon and the total intensity of the magnetic field according to the IGRF model.

2. Imaging riometers

The IRIS instruments at the three stations have almost the similar antenna configurations: a two-dimensional array of 8 by 8 dipole-elements with spacing of a half-wavelength at 38.2 MHz for ZHS/DMH, and with spacing of 0.65-wavelength at 30.0 MHz for NYA. Figure 1 shows the projection of half-power width patterns of 64 antenna-beams on an ionospheric absorption layer at 90 km altitude. The IRIS field-of-view (FOV) is a square of approximately 400 km side and 200 km side for DMH/ZHS and NYA, respectively (Yamagishi *et al.*, 1992).

Figure 2 shows the locations of DMH and NYA and their IRIS FOVs on the European arctic map with invariant latitude contours for 70° and 80°. The north-south direction at DMH, NYA and ZHS IRIS antennas points to the north magnetic pole,

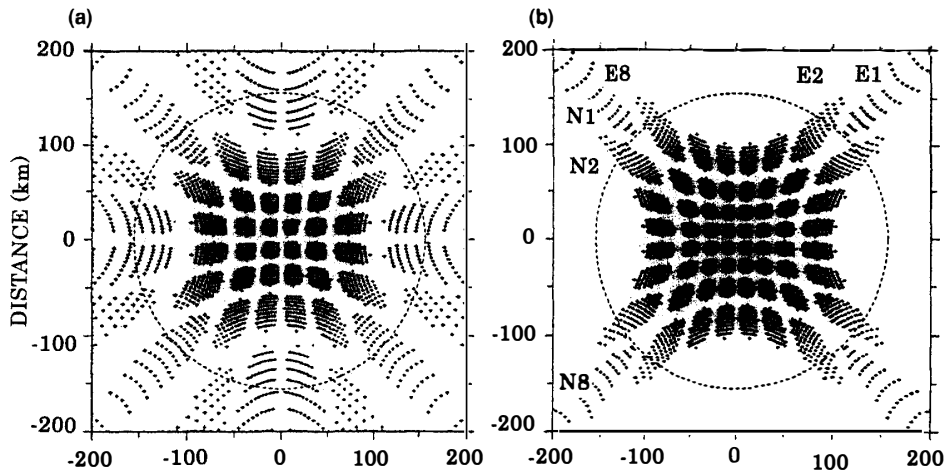


Fig. 1. The projection of a half-power width of 64 antenna-beams on an ionospheric absorption layer at 90 km altitude. The patterns are shown for (a) 0.5-wavelength spacing (Zhongshan/Danmarkshavn IRISs) and (b) 0.65-wavelength spacing (Ny-Ålesund IRIS) (after Yamagishi *et al.*, 1992). The beam numbers noted in the pattern (b) are assigned for north-south and east-west directions.

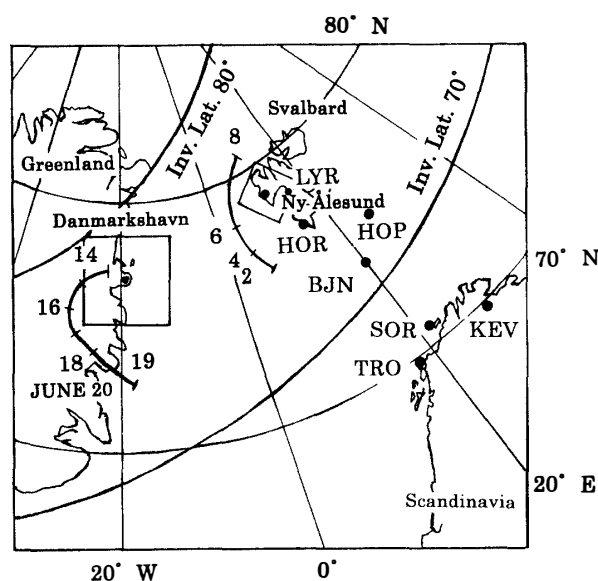


Fig. 2. The IRIS FOVs at Danmarkshavn and at Ny-Ålesund with the invariant latitude contours for 70° and 80° on the European arctic map. Contours giving conjugate locations of Zhongshan are displayed for the morning and afternoon sectors for northern summer solstice (June 20), based on the calculations using the Tsyganenko 1996 model (modified after Yamagishi *et al.*, 1998). The IMAGE magnetometer chain stations extending from Svalbard to northern Scandinavia are also noted by acronyms.

invariant magnetic pole and the south magnetic pole, respectively. Contours giving conjugate locations of ZHS, calculated using the Tsyganenko 1996 model (Tsyganenko and Stern, 1996) under the IMF condition $B_y = B_z = 0$ are also displayed for the morning and afternoon sectors at the northern summer solstice (June 20) (Yamagishi *et al.*, 1998). No conjugate location is obtained between 8 h UT and 14 h UT in the noon sector and between 19 h and 2 h UT in the night sector because of open magnetic field-lines. The locations of IMAGE magnetometer chain stations used in this study are also shown in this figure (Lühr *et al.*, 1998).

3. The daytime absorption event of August 3, 1997

Figure 3 shows time variations of the B_x -, B_y - and B_z -components of the IMF, and ion density (N) and ion dynamic pressure (P_{dyn}) of solar wind from the WIND satellite for the 1030–1400 UT interval of August 3, 1997 in the upper panel, together with absorption variation in the east-west direction near the zenith (S4) at ZHS during 1100–1330 UT in the lower panel. During this interval, the WIND satellite was located at $R_x \sim +80 R_c$, $R_y \sim -60 R_c$ and $R_z \sim +15 R_c$ (in GSE) in the solar wind. The variation of the solar wind dynamic pressure ($P_{\text{dyn}} = mNv^2$) arises almost solely from the ion density. The solar wind dynamic pressure increased from a quiet state (~ 2 nPa) to ~ 6 nPa at 1005 UT, remained at 6–8 nPa (not shown in the panel), and decreased to 6 nPa at about 1100 UT. Thereafter the pressure showed a positive swing ($\Delta P/P \sim 0.6$) which started at 1132 UT, a gradual step-like increase ($\Delta P/P \sim 0.8$) which started at 1150 UT, and a subsequent steep increase

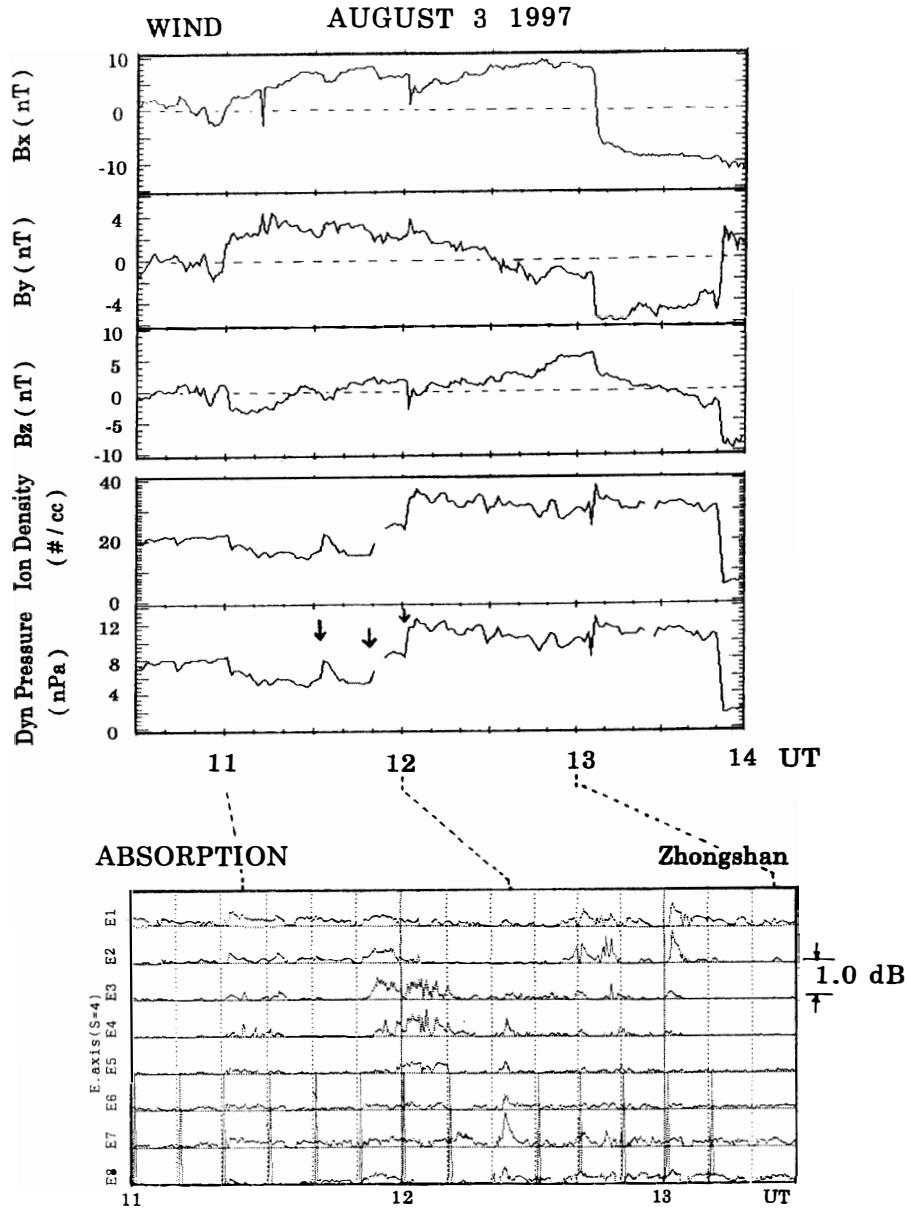


Fig. 3. Time variations of B_x -, B_y - and B_z -components of the IMF, ion density (N) and ion dynamic pressure (P_{dyn}) of solar wind from WIND satellite during 1030–1400 UT on August 3, 1997 (upper panel) together with absorption variation in the east-west direction (E1–E8) near the zenith (S4) during 1100–1330 UT at ZHS (lower panel). Absorption unit is 1.0 dB/div. Dashed lines between the upper and lower panels show the 25-min delay.

($\Delta P/P \sim 1.6$) which started at 1201 UT, followed by a quasi-periodic fluctuation (repetition of ~ 8 min). Between 11 h–13 h UT, B_x was positive with a negative spike at 1201 UT, and B_y was positive with a positive spike at 1201 UT and a gradual negative change at about 1230 UT. B_z gradually changed from negative to positive with a sharp negative spike (peak, -4 nT) at 1201 UT.

To show the relationship between the solar wind conditions and the absorption variation, we estimate a total time delay of 22 min to account for propagation from the satellite to the bow shock ($\sim 12 R_c$) at an average solar wind velocity of 450 km/s, from the bow shock to the magnetopause ($\sim 9 R_c$) and from the magnetopause to the polar ionosphere (Stauning *et al.*, 1995). However, this time delay may be erroneous because the discontinuity in solar wind is not necessarily perpendicular to the sun-earth line. Then we refer to the ground magnetometer data at the low-latitude station Hermanus (geographic lat., -34.4° , long., 19.2°), located on the day side during the present daytime event. Corresponding to the steep pressure increase at 1201 UT, sudden commencement (SC) of the geomagnetic variation started at 1226 UT at Hermanus, which indicates a time delay of 25 min. Dashed lines connecting the panels show the 25-min delay.

Since magnetic noon is approximately 1015 UT at ZHS, the absorption spike event occurred in the post-noon sector (1300–1500 MLT). Unfortunately, strong impulses caused by the calibration signals in the riometer receivers contaminated the absorption variation on the most western beam (E8) every 10 min. Here, we note the absorption spikes corresponding to the solar wind dynamic pressure pulses which started at about 1132 UT, 1150 UT, and 1201 UT, marked by downward arrows. The absorption spikes seen in the eastern beams (E1–E4) around 1152 UT likely correspond to the positive swing pressure of about 1132 UT, followed by fluctuating absorption spikes (E3 and E4) during 1200–1210 UT. The absorption seen only in beam E7 during 1212–1216 UT may correspond to the gradual step-like pressure increase at 1150 UT. The pronounced absorption spike seen in the east-west beams (E3–E8) near 1223 UT clearly corresponds to the steep pressure increase and the synchronous short-period southward IMF change at 1201 UT. The succeeding absorption spikes with a quasi-periodic (QP) feature seen best on beam E7 likely correspond to the pressure oscillation after the steep increase.

Figure 4 shows time variations of the absorption in the east-west direction near the zenith (N4) at DMH and NYA together with those near the zenith (S4) for ZHS shown in Fig. 3. The intensity of absorption spikes at all three stations is mostly below 1 dB. The absorption around 1153 UT at ZHS likely corresponds to very weak absorption (< 0.2 dB) seen in the E2–E6 beams at DMH (shown by broken lines). The absorption enhancement seen only by the E7 beam at ZHS during 1212–1216 UT is probably simultaneous with gradual, weaker absorption in the E2–E6 beams at NYA. By contrast, the pronounced absorption spike seen near 1223 UT at ZHS is clearly identical to the one at NYA (shown by broken lines). The absorption spike at ZHS appears one minute earlier than the one at NYA, and shows eastward motion. The succeeding QP absorption spikes seen best by beam E7 at ZHS are also clearly identical to the spikes for beam E5 or E6 at NYA.

Since during the whole study interval the sun was well below the horizon at Zhongshan, optical aurora observations could be made by all-sky camera. Figure 5 shows a time series of IRIS images of the pronounced absorption spike around 1223 UT (lower panel) and approximately simultaneous aurora all-sky images observed at ZHS (upper panel). Each absorption image shows the average during 32 s. The all-sky camera has panchromatic performance centred at 520 nm wavelength, and thus is most sensitive to green-line emissions produced at about 100 km altitude.

It is quite clear from the absorption images that a small-scale (~ 100 km) absorption enhancement is evident on the western side of the IRIS FOV from 1222:20 UT to 1222:52

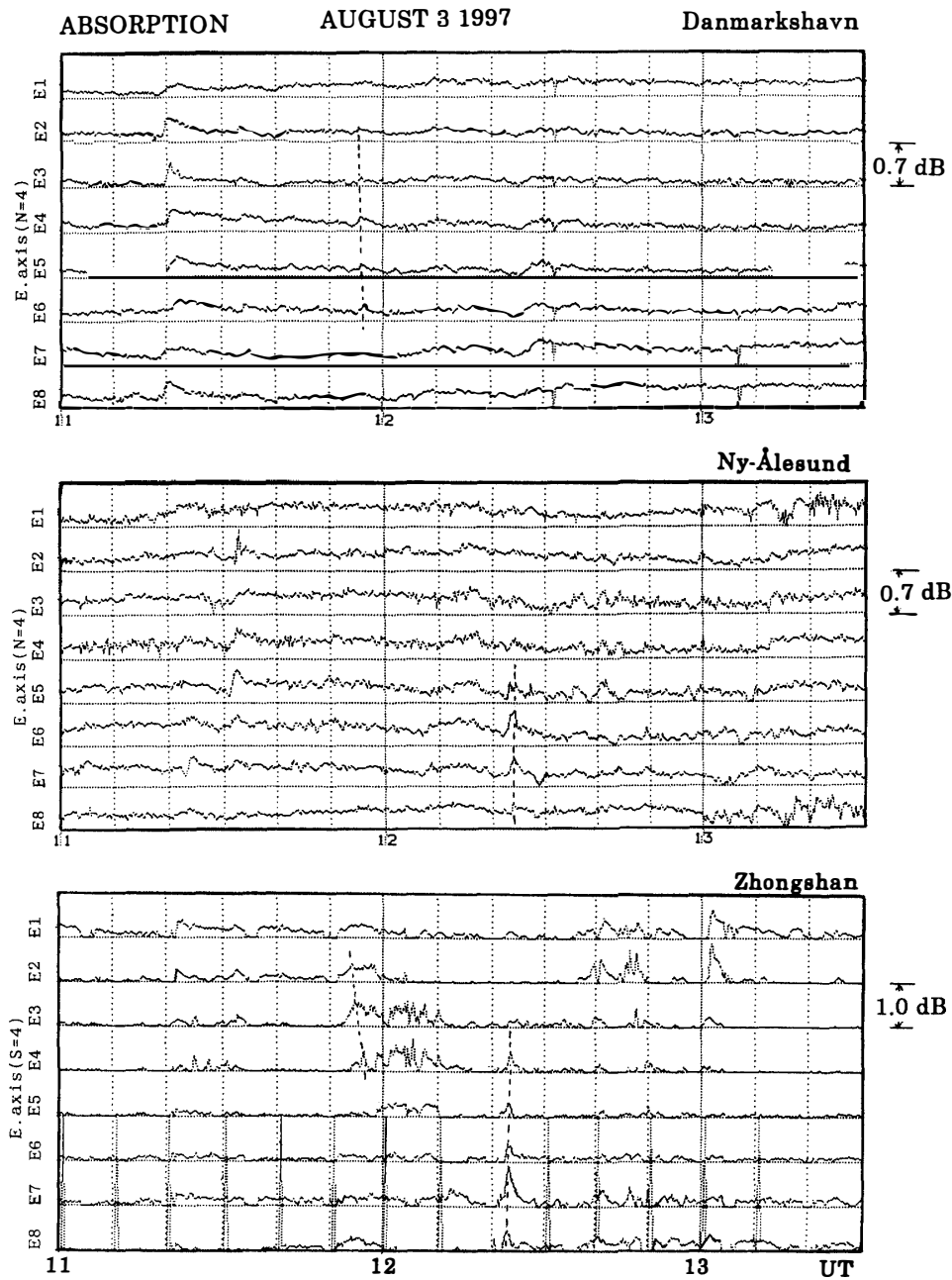


Fig. 4. Time variations of the absorption in the east-west direction near the zenith at DMH, NYA and ZHS during 1100–1330 UT on August 3, 1997. The absorption unit is noted at the right side of the absorption variation, respectively.

UT. Subsequently, the enhancement part moves eastward with a motion of about 3.7 km/s in the large-scale absorption extending exceeding 400 km in longitude and about 50 km in latitude. Maximum absorption (~ 0.9 dB) is found at the western part and near the zenith at 1223:24 UT. Thereafter the absorption activity decreases everywhere. This dynamic behavior is very similar to an auroral arc both in shape and motion (upper panel). However, since the auroral arc is extended in longitude in the whole all-sky FOV, it is

evident deflections for only the initial pressure pulse. Prikryl *et al.* (1998) showed a good correlation between quasi-periodic fluctuations in the solar wind pressure and quasi-periodic convection flow bursts observed by the Iceland HF radars, and also Prikryl *et al.* (1999) showed a good correlation between the riometer absorption fluctuations at Gillam ($\sim 68^\circ\text{N}$) in Canada and the 3–4 min oscillations of the B_y -component during southward IMF. As described above, sudden and fluctuating changes in solar wind dynamic pressure and IMF variation do influence the dynamics of the dayside magnetosphere and thus the high-latitude ionosphere, signifying plasma convection flow bursts, ionospheric current perturbations, and ionospheric absorption increases, as well as aurora activations.

First we discuss a conjugate feature of the absorption spike at about 1223 UT (~ 14 MLT at ZHS) associated with the steep solar wind pressure increase at 1201 UT. Nishino *et al.* (2000) discussed the conjugate relationship between the two hemispheric stations for the same absorption with the one presented in this paper. They have revealed that the conjugate location of ZHS cannot be near 12 h UT under the quiet IMF condition (IMF $B_y = B_z = 0$) due to open magnetic field-lines, as shown in Fig. 2, but could be at the lower-latitude side with eastward displacement under solar wind pressure increase and positive (eastward) IMF- B_y conditions. Here we discuss the time difference of about 1 min between the ZHS and NYA on the absorption spike occurrence near 1223 UT. The IMF B_y changed steeply southward (peak value, -4 nT) with a short period (~ 2 min) at 1201 UT. This IMF change suggests a possibility of transient magnetic reconnection in the lower latitude boundary layer (LLBL) at the duskside magnetopause. Associated with reconnection enhancement, magnetic compressional waves may stimulate magnetospheric electrons on the magnetic shells (Prikryl *et al.*, 1998). If the reconnection occurs in the southern hemisphere, magnetospheric electrons stimulated by the compressional waves may precipitate earlier into the southern hemisphere ionosphere than into the northern hemisphere ionosphere: the absorption spike would appear earlier at the southern hemisphere station (Hargreaves and Chivers, 1965). However, since the B_y orientation is eastward (duskward), it is unreasonable to predict magnetic reconnection in the southern hemisphere. Rather, it may be reasonable to consider that the absorption located in the western region out of the NYA FOV could propagate eastward and reach the NYA station.

Next we discuss plasma sources of the daytime absorption and the mechanism of auroral particle precipitation from the dayside magnetosphere. Nishino *et al.* (2000) found absorption enhancement (~ 1 dB) from the CANOPUS riometer chain in Canada which occurred preceding about one hour from the present absorption spike, and inferred that a population of ample energetic electrons drifting eastward from substorm injection into the nightside magnetosphere would be plasma sources. Another bit of evidence is found from the energy-time spectrogram of electrons (32 eV–32 keV) on the low-altitude DMSP satellite (~ 800 km) (Newell and Meng, 1988). The DMSP satellite passed over the northern part ($\sim 78^\circ\text{N}$) in Greenland at about 1220 UT through the northern area ($\sim 78^\circ\text{N}$) outside Svalbard, and observed precipitations of energetic electron fluxes with a uniform structure in the range above 2 keV during about 1220–1224 UT (not shown here). Thus these observations confirm that plasma sources of the present daytime absorption spikes are high-energy magnetospheric electrons populated in the lower latitude boundary layer (LLBL) at the duskside magnetopause.

In order to examine the magnetic signature for the solar wind pressure variation, we

show the variance of the solar wind pressure exceeding 4 nPa during 1140–1340 UT (upper panel) and the geomagnetic X -components at the IMAGE magnetometer chain stations and at Zhongshan station in Antarctica during 12–14 h UT (lower panel) in Fig. 6. The solar wind pressure variation is shifted by 25 min delay for the ground geomagnetic variation. It is found that the geomagnetic amplitude variation at ZHS is roughly similar to the solar wind pressure variation. It is also found that the geomagnetic amplitude variations are better correlated between ZHS and HOP (or BJJ) than between ZHS and NYA (or LYR). These indicate that the conjugate magnetic signature to the solar wind pressure is most evident between ZHS and HOP (or BJJ) in both hemispheres, which is consistent with the calculation that the conjugate point of ZHS would be located at lower-latitude than NYA under the solar wind pressure increase and eastward IMF- B_y .

Figure 6 also shows that the geomagnetic amplitude peaks at higher-latitude stations than BJJ show a poleward progressing phase with a speed of about 2 km/s, as shown by

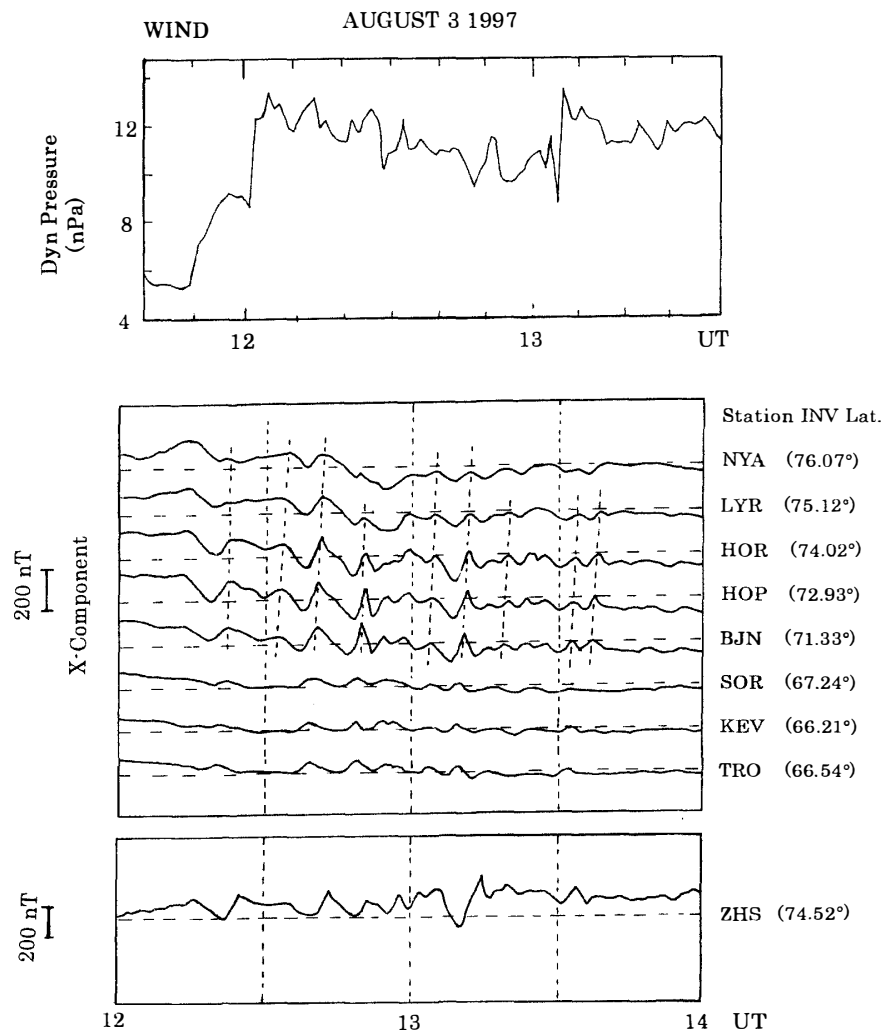


Fig. 6. The variance exceeding 4 nPa of the solar wind dynamic pressure from the WIND satellite (upper panel) and geomagnetic north-south (X) components at the IMAGE magnetometer chain stations and at Zhongshan with invariant latitudes (lower panel). The pressure variation is displayed by 25-min delay for the geomagnetic variation.

some of the broken lines. This feature is in agreement with the variation of the geomagnetic X -components from five high-latitude stations (68.1° – 75.2°), which was indicated as a magnetic signature due to the magnetopause motion associated with the solar wind ram pressure (Farrugia *et al.*, 1989). Prikryl *et al.* (1998) also showed a poleward progressing phase of the geomagnetic X -components from the magnetometer chain on the west coast of Greenland, which was associated with the sudden southward IMF change. They have revealed that the poleward progressing is typical of field line resonance (FLR) in the outer magnetosphere. Although the phase relation between the X -components at ZHS and HOP shows a 2–3 min delay in Fig. 6, it shows near phase agreement between the Y -components at both stations (not shown here). This indicates that the FLR is not determined for the fundamental mode (odd mode) or for the even mode; that is, the two phase relations may be a complicated combination of the FLR effect with the inductive effect of the ionospheric current caused by the enhanced conductivity due to auroral particle precipitations. Further detailed analysis of the phase relation is required.

From the Polar Patrol Balloon experiments near Syowa Station ($L\sim 6$), Antarctica, Hirashima *et al.* (1999) have revealed that compressional MHD waves can produce whistler waves in the outer magnetosphere through electron cyclotron resonance, and result in the identification of pulsating X-rays, Pc5 range ULF pulsations and VLF emissions. The simultaneous identification between riometer absorption and ELF/VLF waves at South Pole station associated with oscillations of the solar wind pressure may indicate that the compressional mode waves would scatter magnetospheric electrons populating in the outer magnetosphere (Sibeck *et al.*, 1989b). Since we have no VLF emission or X-ray data at either hemispheric station, we cannot definitely rule out the mechanism of pitch angle diffusion through electron cyclotron resonance.

However, from statistical analysis of the ground IRIS observations at Sondre Stromfjord (73.7° inv. lat.) in Greenland, Stauning and Rosenberg (1996) have revealed that the high-latitude daytime absorption spikes, typically 0.2–0.3 dB at 38 MHz with spatial extent of 50–100 km, are related to the sudden precipitation of high-energy (30–300 keV) magnetospheric electrons, and may be generated at or a few degrees equatorward of the convection reversal boundary, due to upward region-I FAC intensification in the afternoon convection cell, although they could not determine a definite relationship between the daytime absorption spike events and the solar wind conditions. Sandholt *et al.* (1996) have revealed that the transient form with strong green-line emissions at the equatorward boundary of the preexisting aurora may be explained by the generation of strong, localized field-aligned currents associated with the conversion of a compressional wave into the Alfvén mode at the location of a gradient in the plasma density at the inner edge of the LLBL. Thus it is reasonable to consider that the small-scale enhancement of the absorption showing eastward travel in the large-scale absorption shown in Fig. 5 would be caused by localized energetic electron precipitation due to the formation of field-aligned potential drop between the outer magnetosphere and polar cleft ionosphere.

5. Concluding remarks

We present a post-noon absorption spike event observed by the high-latitude IRIS stations in both the northern and southern hemispheres. Particularly, we examined the

conjugate feature of the absorption spike associated with the steep increase of solar wind pressure and the synchronous southward IMF change, and discussed the mechanism of the energetic particle precipitations including plasma sources. The following concluding remarks emerged from this case study.

- 1) The post-noon absorption spikes with a quasi-periodic feature observed between the conjugate IRIS stations in both the northern and southern hemispheres showed the conjugate ionospheric signature on closed magnetic field-lines.
- 2) The absorption spike showed the small-scale feature with the fast eastward motion in the large-scale absorption extending by about 1000 km in longitude and about 50 km in latitude.
- 3) Magnetic compressional waves driven by the solar wind pressure pulses could stimulate magnetospheric electrons populating in the outer magnetosphere, and the electrons could be precipitated into the cleft ionosphere due to intensification of the strong, localized upward region-1 FAC.

Acknowledgments

We are pleased to acknowledge the encouragement of A. Egeland, University of Oslo. We gratefully acknowledge the Norwegian Polar Research Institute and Chinese Antarctic Expedition for incessant observations at Ny-Ålesund and Zhongshan, respectively, and we greatly appreciate the careful operation of the imaging riometer at Danmarkshavn. We also gratefully acknowledge Ron Lepping, and K. Ogilvie, NASA Goddard Flight Center for supplying the WIND satellite data, P.T. Newell, Johns Hopkins University for supplying the DMSP data. The geomagnetic data at the IMAGE magnetometer stations and at Hermanus station were provided through Web services.

References

- Detrick, D. and Rosenberg, T.J. (1990): A phased-array radio wave imager for studies of cosmic noise absorption. *Radio Sci.*, **25**, 325–338.
- Farrugia, C.J., Freeman, M.P., Cowley, S.W.H., Southwood, D.J., Lockwood, M. and Etemadi, A. (1989): Pressure-driven magnetopause motions and attendant response on the ground. *Planet. Space Sci.*, **37**, 589–607
- Farrugia, C.J., Sandholt, P.E., Cowley, S.W.H., Southwood, D.J., Egeland, A., Stauning, P., Lepping, R.P., Lazarus, A.J., Hansen, T. and Friis-Christensen, E. (1995): Reconnection-associated auroral activity stimulated by two types of upstream dynamic pressure variations: Interplanetary magnetic field $B_z \sim 0$, $B_y \ll 0$ case. *J. Geophys. Res.*, **100**, 21753–21772.
- Glassmeier, K.H. and Heppner, C. (1992): Traveling magnetospheric convection twin vortices: Another case study, global characteristics, and a model. *J. Geophys. Res.*, **97**, 3977–3992.
- Hirashima, Y., Simobayashi, H., Yamagishi, H., Suzuki, H., Murakami, H., Yamada, A., Yamagami, T., Namiki, M. and Kodama, M. (1999): MHD wave characteristics inferred from correlations between X-ray, VLF, and ULF's at Syowa Station, Antarctica and Tjörnes, Iceland ($L \sim 6$). *Earth Planet. Sci.*, **51**, 33–41.
- Hargreaves, J.K. and Chivers, H.J.A. (1965): A study of auroral absorption events at the South Pole, 2. Conjugate properties. *J. Geophys. Res.*, **70**, 1093–1102.
- Lühr, H., Aylward, A., Bucher, S.C., Pajunpaa, K., Holmboe, T. and Zalewski, S.M. (1998): Westward moving dynamic substorm features observed with the IMAGE magnetometer network and the ground-based instruments. *Ann. Geophys.*, **16**, 425–440.
- Mende, S.B., Rairden, R.L., Lanzerotti, L.J. and MacLenman, C.G. (1990): Magnetic impulses and

- associated optical signatures in the dayside aurora. *Geophys. Res. Lett.*, **17**, 131–134.
- Newell, P.T. and Meng, C.-I. (1988): The cusp and the cleft/boundary layer: Low altitude identification and statistical local time variation. *J. Geophys. Res.*, **93**, 14549–14556.
- Nishino, M., Tanaka, Y., Oguti, T., Yamagishi, H. and Holtet, J.A. (1993): Initial observation results with imaging riometer at Ny-Ålesund ($L=16$). *Proc. NIPR Symp. Upper Atmos. Phys.*, **6**, 47–61.
- Nishino, M., Yamagishi, H., Sato, N., Sanoo, Y., Ruiyuan, L., Honquao, H. and Stauning, P. (1998): Initial results of imaging riometer observations at polar cap conjugate stations. *Proc. NIPR Symp. Upper Atmos. Phys.*, **12**, 58–72.
- Nishino, M., Yamagishi, H., Sato, N., Liu, R., Hongquao, Hu., Stauning, P. and Holtet, J.A. (2000): Conjugate features of daytime absorption associated with specific changes in the solar wind observed by inter-hemispheric high-latitude imaging riometers. *Adv. Polar Upper Atmos. Res.*, **14**, 76–92.
- Prikryl, P., Greenwald, R.A., Sofko, G.J., Villain, J.P., Ziesolleck, C.W.S. and Friis-Christensen, E. (1998): Solar-wind-driven pulsed magnetic reconnection at the dayside magnetopause, Pc5 compressional oscillations, and field line resonances. *J. Geophys. Res.*, **103**, 17307–17322.
- Prikryl, P., Macdougall, J.W., Grant, I.F., Steele, D.P., Sofko, G.J. and Greenwald, R.A. (1999): Observations of polar patches generated by solar wind Alfvén wave coupling to the dayside magnetosphere. *Ann. Geophys.*, **17**, 463–489.
- Sandholt, P.E., Farrugia, C.J., Burlaga, L.F., Holtet, J.A., Moen, J., Lybekk, B., Jacobsen, B., Opsvic, D., Egeland, A., Lepping, R., Lazarus, A.J., Hansen, T., Brekke, A. and Friis-Christensen, E. (1994): Cusp/cleft aurora activity in relation to solar wind dynamic pressure, interplanetary magnetic field B_z and B_y . *J. Geophys. Res.*, **99**, 17323–17342.
- Sandholt, P.E., Farrugia, C.J., Stauning, P., Cowley, S.W.H. and Hansen, T. (1996): Cusp/cleft auroral forms and activities in relation to ionospheric convection: Responses to specific changes in solar wind and interplanetary magnetic field conditions. *J. Geophys. Res.*, **101**, 5003–5020.
- Sibeck, D.G., Baumjohann, W. and Lopez, R.E. (1989a): Solar wind dynamic pressure variations and transient magnetospheric signatures. *Geophys. Res. Lett.*, **16**, 13–16.
- Sibeck, D.G., Baumjohann, W., Elphic, R.C., Fairfield, D.H., Fennel, J.F., Gail, W.B., Lanzerotti, L.I., Lopez, R.E., Luehr, H., Lui, T.Y., MacLennan, C.G., McEntire, R.W., Potemra, T.A., Rosenberg, T.J. and Takahashi, K. (1989b): The magnetospheric response to 8-minute period strong-amplitude upstream pressure variations. *J. Geophys. Res.*, **94**, 2505–2519.
- Stauning, P. and Rosenberg, T.J. (1996): High-latitude daytime absorption spike events. *J. Geophys. Res.*, **101**, 2377–2396.
- Stauning, P., Henriksen, S. and Yamagishi, Y. (1992): Imaging riometer installation in Danmarkshavn, Greenland. Danish Meteorological Institute, Technical Report, **92-4**, 1–25.
- Stauning, P., Clauer, C.R., Rosenberg, T.J., Friis-Christensen, E. and Sitar, R. (1995): Observations of solar-wind-driven progression of interplanetary magnetic field B_z -related dayside ionospheric disturbances. *J. Geophys. Res.*, **100**, 7567–7585.
- Tsyganenko, N.A. and Stern, D.P. (1996): Modeling the global magnetic field of the large-scale Birkeland current systems. *J. Geophys. Res.*, **101**, 27187–27198.
- Yamagishi, H., Nishino, M., Sato, M., Kato, Y., Kojima, M., Sato, N. and Kikuchi, T. (1992): Development of imaging riometers. *Nankyoku Shiryo* (Antarct. Rec.), **36**, 227–250 (in Japanese with English abstract).
- Yamagishi, H., Fujita, Y., Sato, N., Stauning, P., Nishino, M. and Makita, K. (1998): Conjugate features of auroras observed by TV cameras and imaging riometers at auroral and polar cap conjugate-pair stations. *Polar Cap Boundary Phenomena*, ed. by J. Moen *et al.* Dordrecht, Kluwer Academic Publ., 289–300 (NATO ASI Ser.; Ser. C 509).

(Received June 2, 2000; Revised manuscript accepted November 6, 2000)